Archive of Applied Mechanics (2021) 91:3679–3692
https://doi.org/10.1007/s00419-021-01915-3

ORIGINAL

Daniel Müller · Jens Stahl · Anian Nürnberger · Roland Golle · Thomas Tobie · Wolfram Volk · Karsten Stahl

Shear cutting induced residual stresses in involute gears and resulting tooth root bending strength of a fineblanked gear

Received: 9 October 2020 / Accepted: 10 February 2021 / Published online: 26 February 2021

Abstract The manufacturing of case-hardened gears usually consists of several complex and expensive steps to ensure high load carrying capacity. The load carrying capacity for the main fatigue failure modes pitting and tooth root breakage can be increased significantly by increasing the near surface compressive residual stresses. In earlier publications, different shear cutting techniques, the near-net-shape-blanking processes (NNSBP's), were investigated regarding a favorable residual stress state. The influence of the process parameters on the amount of clean cut, surface roughness, hardness and residual stresses was investigated. Furthermore, fatigue bending tests were carried out using C-shaped specimens. This paper reports about involute gears that are manufactured by fineblanking. This NNSBP was identified as suitable based on the previous research, because it led to a high amount of clean cut and favorable residual stresses. For the fineblanked gears of S355MC (1.0976), the die edge radii were varied and the effects on the cut surface geometry, hardness distribution, surface roughness and residual stresses are investigated. The accuracy of blanking the gear geometry is measured, and the tooth root bending strength is determined in a pulsating test rig according to standardized testing methods. It is shown that it is possible to manufacture gears by fineblanking with a high precision comparable to gear hobbing. Additionally, the cut surface properties lead to an increased tooth root bending strength.

Keywords Gears · Shear cutting · Near-net-shape blanking · Residual stresses · Fatigue testing · Tooth root breakage · Tooth root bending strength

1 Introduction

Fineblanking is a mechanical separation process, which is able to produce smooth cut surfaces without a fracture zone, a small die roll, and thus a high amount of clean cut. Compared to the commonly used standard shear cutting process, this is achieved by a special tool setup consisting of a v-ring on the die and/or blank holder plate, and a counter punch as illustrated in Fig. 1.

Due to the high amount of clean cut, which can act as a load bearing surface, fineblanking is used for manufacturing precision parts like gears. Fineblanked gears are widely used for example in cars or medical equipment [8]. Due to the relevance of the clean cut in these applications, many research works deal with its improvement by adjusting the fineblanking process parameters.

The most important process parameter is the die clearance, the horizontal distance between punch and die [34]. It is often given as a percentage of the sheet metal thickness and is therefore referred to as relative die

D. Müller (✉) · T. Tobie · K. Stahl
Institute of Machine Elements (FZG), Technical University of Munich, Boltzmannstraße 15, 85748 Garching, Germany
E-mail: mueller@fzg.mw.tum.de

J. Stahl · A. Nürnberger · R. Golle · W. Volk
Chair of Metal Forming and Casting (utg), Technical University of Munich, Walther-Meissner-Straße 4, 85748 Garching, Germany

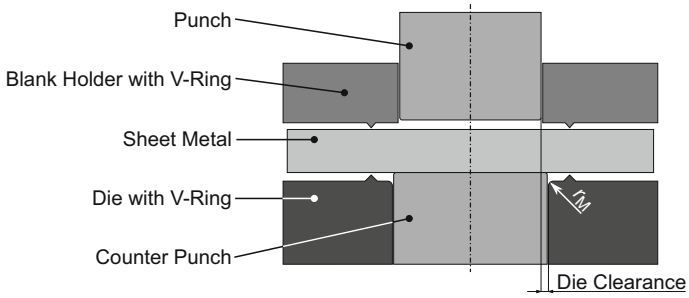

Fig. 1 Typical tool setup of fineblanking

clearance. Spišák et al. found that a small die clearance is beneficial when a high amount of clean cut is of interest [28]. A value of 0.5% is recommended in Schmidt et al. [26]. This was confirmed for example by Su et al. [33]. Another process parameter is the preparation of the punch and die geometry. As stated in Klocke et al. [19], either the punch or the die edge should be rounded when a high amount of clean cut is desired. Kim et al. found that a chamfer with an angle of 30° or 45° to the sheet metal plane should be preferred to an angle of 60° when the chamfer width is kept constant [17]. The v-ring geometry and position influence has been investigated in [6]. It was found that a v-ring with a tip angle of 90° and a distance of approximately 3 mm to the cutting line is suitable to achieve a high amount of clean cut.

Not only the geometry, i.e., the clean cut height, is of interest but also the ability of the manufactured part to withstand the different load cases it is subjected to in gear applications. The main fatigue failures of gears are tooth root breakage, pitting and tooth flank fracture (TFF). Pitting and tooth root breakage are usually initiated at the surface or close to the surface, whereas TFF is initiated in larger material depths. Pitting begins with crack initiation near the flank surface and results in the formation of small pits on the tooth flank. Tooth root breakage is characterized by a crack initiation at the surface close to the contact point of the 30°-tangent to the tooth root fillet. The crack then propagates in direction of the tooth root at the opposite site of the tooth until breakage. These failures are covered by the standardized rating procedures according to ISO 6336 [13], respectively, DIN 3990 [4].

There are no publications known to the authors that cover the fatigue properties of gears manufactured by fineblanking or shear cutting. Consequently, no gear strength numbers are available. Only basic research on simple geometries has been carried out that deals with the fatigue strength of shear cut edges in general. For example, Lara et al. and Maronne et al. found that a small die clearance is beneficial [20,21]. In earlier works of the presenting authors, it was shown that the chosen shear cutting process influences the part's residual stress state [30] which significantly alters the resulting fatigue strength [29]. Here, we were able to show that higher shear cutting-induced compressive residual stresses are able to increase the part fatigue strength. Similar observations were made for subsequent residual stress alteration by coining published by Yasutomi et al. [40].

As there are no publications present that deal with the highly relevant gear failure mode "tooth root breakage" of shear cut gears, the influencing factors are given in hereinafter for gear hobbing. This is extended by an insight on how the respective property can be adjusted by fineblanking.

Today's demands on power transmitting gears are high and damages, especially breakages must be strictly avoided in most applications. For case-hardened gears, the main failure modes are well researched and the main influences are known. Main influences on tooth root breakage are for example the material, the hardness depth profile, the residual stresses. [24]

To achieve higher power density, a gear has to be manufactured with optimal properties to ensure higher load carrying capacity. In addition, the reduction of weight as well as costs play an important role.

The manufacturing process consists of several complex and costly steps. Usually, an involute gear geometry is manufactured by gear hobbing. At first, the involute teeth are milled by a gear hobbing cutter. After the macro-geometry is completed, a heat treatment process is applied to increase the strength of the gear. Afterward, a grinding process is usually necessary at the gear flank to compensate hardening distortions and/or to apply a specific micro-geometry to ensure a favorable load distribution. [24]

Optionally, further treatments such as shot-peening or barrel finishing are applied. Barrel finishing after grinding reduces the roughness and therefore decreases the risk of pitting failure of the gear. A shot peening process before grinding usually increases the near surface residual stresses and therefore has significant impact

Table 1 Measured chemical composition of the sheet metal material S355MC in percentage by mass [23]

Element	C	Mn	Si	P	S	Al_{Ges}	Nb	V	Ti
wt%	0.06	0.503	< 0.01	0.014	0.007	0.019	0.023	< 0.002	< 0.001

on the pitting strength when applied on the tooth flank. By shot peening of the tooth root, the tooth root bending strength increases significantly. [7]

A case carburizing process for gears made of commonly used materials, such as 20MnCr5 or 18CrNiMo7-6, can lead to compressive residual stresses at the surface around up to ca. -300 MPa for depending on the case hardening depth (CHD) and further influencing factors. A shot peening process after the heat treatment can increase compressive residual stresses up to ca. −1200 MPa. The increase in tooth bending strength after shot peening is depending on many influencing factors but an increase up to ca. 40% compared to the unpeened condition is stated in various researches such as in [37]. In [7], an increase in tooth root bending strength over 50% compared to the unpeened condition was stated. The surface hardness is also a main influencing factor on the tooth root bending strength. Up to a surface hardness of ca. 500 HV, the tooth bending strength increases linearly [24].

It has been shown by Thipprakmas et al. [35] that a significant hardness increase by strain hardening is present in fineblanked parts. This hardness distribution can be controlled within a small range by the blank holder and counter punch force, for example. The presenting authors already were able to show, that the residual stress state can be controlled by adjusting punch and die edge radii. A rounder punch edge leads to higher compressive residual stresses in fineblanked holes compared to a sharp punch edge [23]. Česnik et al. [1] stated that the control of the residual stress state is also necessary to achieve a high part precision.

Fineblanked gears could be used for applications, where lower torques are transmitted and case-hardened gears are too expensive. In these applications, mainly plastic gears are used at the moment, which allow a cost-efficient mass production with injection molding. In this process, the plastic gear rim is applied on a steel insert. However, the load carrying capacity of these gears is very low compared to case-hardened gears. In addition, the load carrying capacity is strongly dependent on the temperature, which limits the field of applications. These gears cost roughly 10% of a steel gear but have the advantage of being around 30% less heavy. [38]

The herein proposed blanking process for involute gears is very cost efficient for mass production and a high power density could be achieved by using the positive effect of the process-induced residual stresses. Furthermore, the manufacturing process could be used for further applications, where a high strength functional surface is necessary such as in cyclodrive disks. This publication provides a first investigation of involute gears manufactured by fineblanking. We combine the findings in our previous publications, i.e., that compressive residual stresses increase the fatigue strength of simple fineblanked parts [29], with the findings presented by [7] that the fatigue strength of gear wheels can be increased by compressive residual stresses. Thus, the central aim of this paper is the achievement of a high compressive residual stress state in the region of interest by adjusting the fineblanking process parameters. As this alone is not relevant for industrial applications, we additionally determined the strength numbers according to ISO 6336-5 [15]. Based on these strength numbers, applications for the gears can be chosen by the transmission producers.

2 Experimental setup and test equipment

2.1 Material

The gears were manufactured out of the micro-alloyed, finegrained, hot-rolled structural steel S355MC (1.0976). The sheet metal thickness is 6 mm. The austenite free S355MC is a typical steel used in fineblanking and was also used in previous publications of this research project [29,30]. Its chemical composition was measured with an optical emission spectrometer and is listed in Table 1. The mechanical properties were measured in [23,30], where the tensile strength is stated ca. 485…496 MPa and the yield strength ca. 418…438 MPa depending on the rolling direction.

Table 2 Gear geometry of C-PT-gearing

Denomination	Symbol	Pinion	Wheel
Number of teeth	z_1, z_2	16	24
Normal module	m_n	4.5 mm	
Center distance	a	91.5 mm	
Normal pressure angle	α_n	20°	
Helix angle	β	0°	
Facewidth	b	6 mm*	
Profile shift coefficient	x_1, x_2	0.1817	0.1716
Tip diameter	da_1, da_2	82.45 mm	118.35 mm

*Adjusted for the herein investigated fineblanked gears

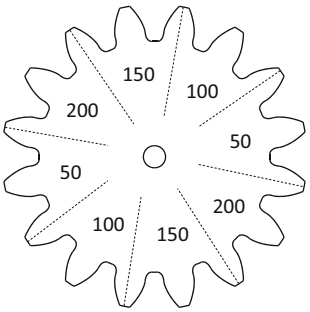

Fig. 2 Classification of zones with different die edge radii on the fineblanked gear

2.2 Investigated gear geometry

The gear geometry has been chosen in order to be able to test both tooth bending strength and pitting strength. Therefore, a test gearing for pitting strength tests (FZG Type C-PT) was selected and the facewidth b of the gearing was adjusted for the herein investigated fineblanked gears. The test gearing is usually investigated in a standardized running test rig (FZG back-to-back test rig). However, the gears can also be tested for tooth bending strength in a pulsating test rig such as in [27]. For the herein presented research, the pinion of the gearing shown in Table 2 was manufactured and tested regarding tooth root bending strength.

2.3 Shear cutting tool

The gears were manufactured by fineblanking with a triple-action fineblanking press Feintool HFA 3200 plus with a nominal press force of 3200 kN. A constant die clearance of 0.5% (30 μm) was manufactured. A circular v-ring (diameter 88.4 mm) on blank holder plate and die plate was chosen with a geometry as published in [30]. The blank holder force was set to 611 kN and the counter punch force to 291 kN. Thus, the same force per v-ring length and the same counter punch pressure as in the last publications [29,30] was achieved. A typical punch velocity for industrial applications of 50 mm/s was chosen.

The punch was ground to show a sharp punch edge of less than 20 μm. Only on the sharp radii of the tooth head, a small radius of 50 μm was polished to the edge to prevent the cutting edge from breaking. The die was polished to show different radii r_M as displayed in Fig. 2. Thus, the blanked pinion is divided into 8 parts with 4 different die edge radii $r_M = 50, 100, 150, 200\,\mu$m. The symmetry of this polishing strategy prevents uneven lateral forces which may affect the precision. Additionally, this allows to measure and test at least two tooth roots on each side for each die edge radius.

2.4 Residual stress measurements

The surface residual stresses were measured with a PULSTEC μ-$X360s$ portable X-ray diffractometer. A 1 mm collimator hole was used to measure the residual stresses with a chromium X-ray tube type in the ferrite plane (211). The residual stresses are then evaluated with $cos\,\alpha$-method. The gear was not cut before these

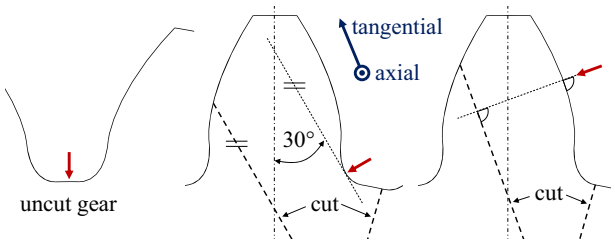

Fig. 3 Residual stress measurement points on the gears (arrows): the measurement of axial residual stresses at the uncut gear and the measurements of tangential and axial residual stresses depth profiles on the cut gear tooth at the contact point of the 30°-tangent and at the tooth flank

measurements. The surface residual stresses in axial direction (sheet thickness direction) were measured in the middle of the tooth ground (see Fig. 3) because measurement at the critical section for tooth root breakage (contact point of the 30°-tangent) was not possible without cutting of the gear. Residual stresses in axial direction were measured for all 4 variants 6 times and then the mean value with the standard deviation is calculated. As this measurement is not affected by a subsequent cutting operation, it is very well suited to identify the influence of the fineblanking process parameters on the residual stress state. To get a robust result, these measurements are carried out in the tooth root, where the geometry is comparably easy. Nevertheless, as etching and tangential measurements are not possible due to the geometry restrictions, this measurement offers limited but precise information.

The surface residual stress as well as the residual stresses depth profiles were also measured with a Seifert XRD 3003 PTS System with Cr-Kα radiation. A 1 mm collimator was used and is positioned in the middle of the sheet thickness (middle of tooth facewidth) with 10 mm distance between collimator and specimen surface. The residual stresses were evaluated with the $\sin^2\psi$-method. The measurement was previously described in [30]. The electrochemical erosion (etching) was performed with NaCl as electrolyte. The tangential and axial residual stresses were measured at the contact point of the 30°-tangent to the tooth root fillet and on the flank at half tooth height as shown in Fig. 3. For these measurements, the tooth was cut with a cutting disk and separated from the gear. The cut was placed ca. 1 mm from the measuring point at the contact point of the 30°-tangent in the tooth root as shown in Fig. 3. The cutting was performed with sufficient cooling, therefore influences of the heat on the residual stresses can be ruled out. Influences of the cutting on the residual stresses have so far not been observed for higher-strength materials such as case-hardened materials [32]. However, for this lower strength material a stress relief due to the cutting is conceivable. Thus, these measurements offer detailed information on the residual stress state in the region of interest. Nevertheless, it is more error prone as the cutting of the specimens can be expected to influence the results. The flank measurements allow to interpret the influence of the cutting line geometry, i.e., the geometry influence of the fineblanking process.

2.5 Further measurement methods

The fineblanked gear geometry was further investigated regarding cut surface characteristics, hardness, surface roughness and geometric manufacturing accuracy. The cut surface characteristics were measured by a tactile surface measuring station MarSurf PCV. The hardness distribution (HV0.2) was measured with a LECO AMH-43 micro-hardness tester. The gear geometry was measured with a 3D gear measuring center (P40 Klingelnberg).

2.6 Fatigue testing—tooth root bending strength

The tooth bending strength can be tested in a running test rig whereby pinion and wheel are necessary, which leads usually to higher testing costs. A more cost-efficient and commonly used testing method is the testing of a reference gear in a pulsating test rig. Additionally, multiple tests can be performed with a single gear. The determined strength of the pulsating tests can be transferred to strength numbers for running tests [5].

The fatigue testing regarding tooth root breakage for this paper was performed in a pulsating test rig according to the standards of FVA Directive 563 I [36]. The test gears are symmetrically clamped over $k = 3$ teeth between two plane-parallel jaws. The exact position of the test gear in relation to the clamp jaws is adjusted

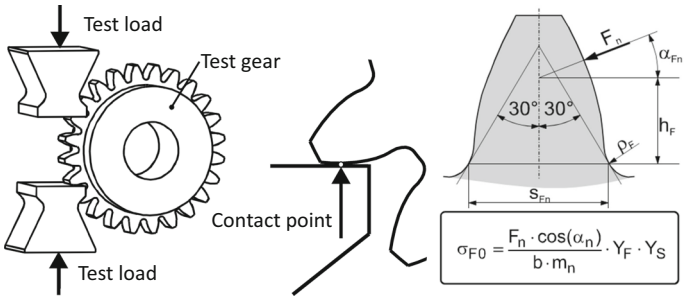

Fig. 4 Clamping of the gear in the pulsating test rig and calculation of nominal tooth root stress σ_{F0} according to ISO 6336-3 and DIN 3990. [10]

by means of a special jig. Flank angle deviations are compensated by means of a precision adjustment, so that a uniform load distribution across the whole tooth facewidth was ensured [5]. A schematic representation is given in Fig. 4.

The teeth of the pinion were loaded with tensile swelling loads at a test frequency of 50 Hz. The lower load limit of the swelling load is 0.5 kN to hold the gear, which is 5…10% of the upper load and therefore the influence of the clamping force on the test results is negligible [36].

The nominal tooth bending stress σ_{F0} is calculated according to the standards DIN 3990-3 and ISO 6336-3 as shown in Fig. 4 with consideration of the actual geometry of the manufactured gear within the stress factor Y_S and form factor Y_F.

To determine the tooth bending strength number the endurance limit has to be determined. For the standard test procedure, there is a maximum number of load cycles of 6 M, which has to be reached in order to classify the test as passed in the high cycle fatigue regime. The staircase evaluation method according to Hück [11] is used to determine the endurance limit, respectively, the tooth root fatigue strength values with at least 12 test runs. Additional 10 tests are carried out in the limited lifetime on two pulsating force load stages to determine the standard allocation S–N curve (Wöhler-curve) for 50% failure probability according to [36]. The limited lifetime is evaluated according to Haibach [9].

After the calculation of the nominal tooth bending stress σ_{F0}, the tooth root fatigue strength values for the tested gears can be determined according to ISO 6336-3 [14]. To calculate the safety factors of a gearing against tooth root breakage, the strength numbers in ISO 6336-5 [15] are usually used. For the calculation of gears with new materials, these strength numbers are usually determined based on the results in pulsating test rigs.

With Eq. 1, the nominal strength number σ_{Flim} for bending is calculated based on the manufactured gear (factors shown in Table 5) and the determined endurance limit for 50% failure probability $\sigma_{F0\infty,50\%,\mathrm{pulsator}}$. The relative notch sensitivity factor $Y_{\delta \mathrm{rel}T}$ and the relative surface factor $Y_{R\mathrm{rel}T}$ are factors depending on the properties of the gear. As well as the stress correction factor Y_{ST} and the size factor Y_X, which for example, takes into account the gear size compared to a module 5 mm standard reference gear. For the conversion from pulsator test results to running test results, the factor $f_P = 0.90$ is used and for the conversion from 50% failure probability to 1% failure probability the factor $f_{1\%F}$ is applied [25]. The life factor Y_{NT} is set to 1.0 according to ISO 6336-3 [14].

$$\sigma_{\mathrm{Flim}} = \frac{\sigma_{F0\infty,50\%,\mathrm{pulsator}} \cdot f_P \cdot f_{1\%F}}{Y_{\delta \mathrm{rel}T} \cdot Y_{R\mathrm{rel}T} \cdot Y_{\mathrm{NT}} \cdot Y_X \cdot Y_{\mathrm{ST}}}. \tag{1}$$

For the calculation of the allowable stress number for bending, Eq. 2 is used.

$$\sigma_{\mathrm{FE}} = Y_{\mathrm{ST}} \cdot \sigma_{\mathrm{Flim}}. \tag{2}$$

3 Results and discussion

3.1 Cut surface characteristics

The cut surface characteristics of the manufactured sections measured in the tooth root fillet are shown in Fig. 5. Although the die edge radius is varied in a comparable big range, only small changes can be observed.

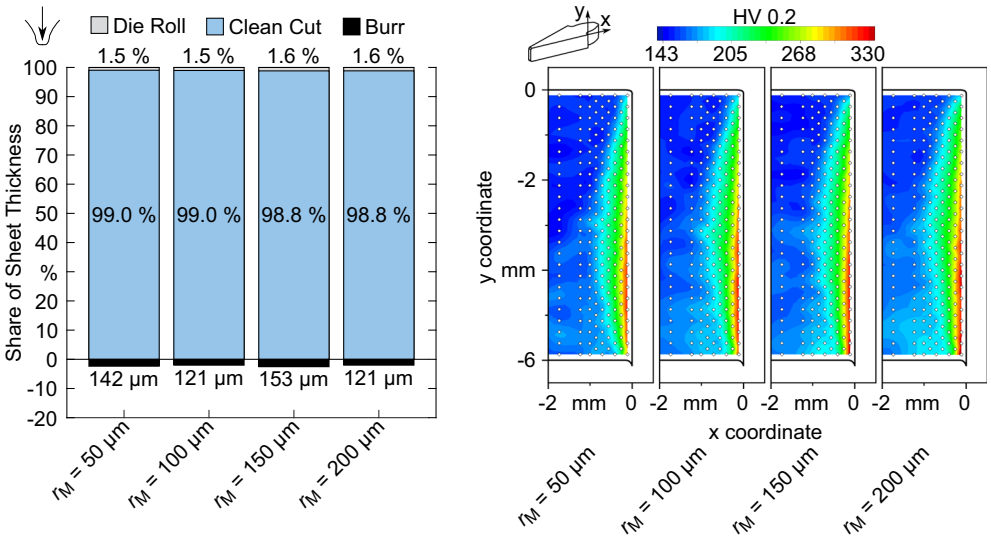

Fig. 5 Cut surface characteristics in the tooth root for the four different die edge radii r_M (left) and the corresponding HV0.2 hardness distributions (right)

Table 3 Cut surface roughness Ra and Rz in μm of the fineblanked gears

r_M in μm	Ra in μm	Rz in μm
50	1.36	8.30
100	1.55	9.46
150	1.65	8.84
200	1.77	10.4

A fracture zone is not present for all die edge radii. The die roll ranges between 1.5 and 1.6%. Consequently, a big clean cut portion of 98.8–99.0% is observed, where the small radii of 50 μm and 100 μm show a slightly higher clean cut share. No clear trend is visible for the burr height, which varies between 121 and 153 μm.

The hardness in the tooth root is also displayed in Fig. 5. A significant hardness increase by the shear cutting-induced strain hardening is present, which changes the materials hardness from 153 HV0.2 inside the sheet metal to over 328 HV0.2 on the clean cut. Again, no clear trend is visible for the four die edge radii. Only close to the burr, a higher hardness can be observed when a bigger die edge radius is chosen.

The arithmetical mean deviation Ra and the maximum height Rz of the assessed roughness profile are investigated according to [12]. The surface roughness was measured in tangential direction at the tooth flank. The roughness in the tooth root is expected to be comparable. The results are shown in Table 3. In particular, for Ra a clear trend is visible, where a bigger die edge radius leads to a higher roughness.

3.2 Gear geometry and gear quality

The gear geometry was measured with the gear measurement center. For the four variants, a contourscan was performed in the middle of the sheet thickness of the cut surface as well as near the edges at ca. 0.1 mm distance from top or bottom of the sheet. The measurements on the different positions over the sheet thickness show comparable results. Furthermore, the individual variants show comparable results. A comparison for the variant $r_M = 50\,\mu$ m is shown in Fig. 6. It can be seen that high conformity was accomplished and the largest deviation is at the radius of the tooth tip, which has no effect on the tooth bending strength or pitting strength of the gear. However, manufacturing of sharper edges is possible with this fineblanking technique but was not attempted for this research.

The predefined geometry, which is based on gear hobbing tool parameters and the measured geometry were compared based on the geometrical parameters stated in ISO 6336-3 [14], which are the gear tool parameters defined in DIN 3960 [2] such as the tip diameter d_A, radius coefficient of tool tip ρ_{aP0^*}, generating profile shift x_E.

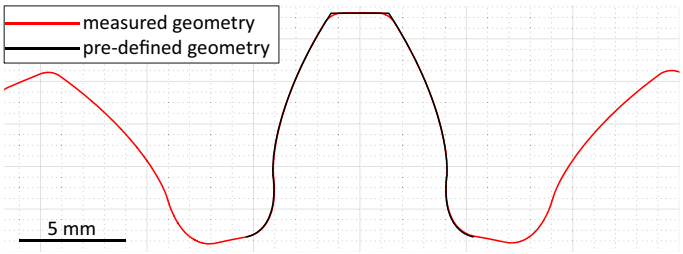

Fig. 6 Comparison of predefined and measured geometry

Table 4 Tooth bending strength calculation factors Y_F and Y_S of the manufactured geometry for the 4 different die edge radii

r_M in μm	Y_F	Y_S
50	1.793	1.949
100	1.783	2.002
150	1.769	2.018
200	1.771	2.020

For the calculation of the tooth bending strength according to ISO 6336-3 [14], the different tool parameters of the manufactured geometry are mandatory for the calculation of the nominal tooth root stress. These factors such as the normal chordal dimension s_{Fn}, the bending moment arm h_{Fe}, the stress factor Y_S and the form factor Y_F are determined based on the measurements with the gear measurement center.

All three measurements on different positions over the sheet thickness show comparable values for a die edge radius. The mean values of the three measurements are shown in Table 4 for clamping over $k = 3$ teeth. In addition, all four different die edge radii show a high conformity with the predefined geometry and all values are comparable.

The gear geometry was also measured with the gear measurement center to investigate the accuracy rate or quality grade of the gear geometry. Three teeth ($r_M = 50, 100, 200\,\mu$m) of a gear were measured. The teeth show comparable geometrical results. The measured tooth trace is in good agreement with the involute form. However, at the tip area a larger deviation is observed due to the round tip edges, which is comparable to a larger tip relief.

The quality grade according to DIN 3962 [3] is determined based on mean values of the 3 teeth. According to DIN 3962, a quality grade of 4…7 depending on the investigated geometrical parameter could be reached. The pitch deviation is $F_r = 17.2\,\mu$m, which corresponds to quality grade 6 [3]. Therefore, the quality grade of the manufactured fineblanked gear is in the range of milled and case-hardened gears after grinding of the gear.

3.3 Process-induced residual stresses

The surface axial residual stresses of the four variants with a standard deviation from the six measurements per variant are shown in Fig. 7. For these measurements, no cutting of the tooth was performed, which would be only needed for the residual stresses in tangential direction or for the etching process for the measurement of depth profiles. It is clearly visible that a larger die edge radius leads to higher compressive residual stresses. However, the standard deviation of the six measurements is between 70 and 120 MPa.

In Fig. 8, the residual stress depth profiles are shown for teeth cut with the four different die edge radii. The surface residual stresses are measured at the contact point of the 30°-tangent and the depth direction is normal to the surface. The axial residual stress measurements show a transition from compressive to tensile stresses in a depth of ca. 0.05 mm for all variants. In larger material depths, the axial tensile residual stresses are in the range of ca. 100…200 MPa. For the tangential residual stresses, the transition from compressive to tensile stresses is closer to the cut surface compared to the axial residual stresses. In larger material depths, the tangential tensile residual stresses are mostly higher than the axial residual stresses.

At the surface (contact point of the 30°-tangent to the tooth root fillet), the axial compressive residual stresses seem to decrease with larger die edge radius from ca. −400 to −250 MPa, which does not correlate with the surface measurements in the tooth ground of the uncut gear. The tangential (in direction of tooth height) surface residual stresses also show no correlation with the die edge radius. For $r_M = 50\,\mu$m and

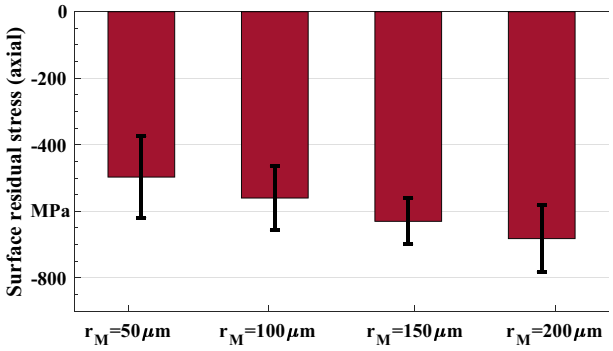

Fig. 7 Results of surface axial residual stress measurements in the tooth ground of the uncut gear

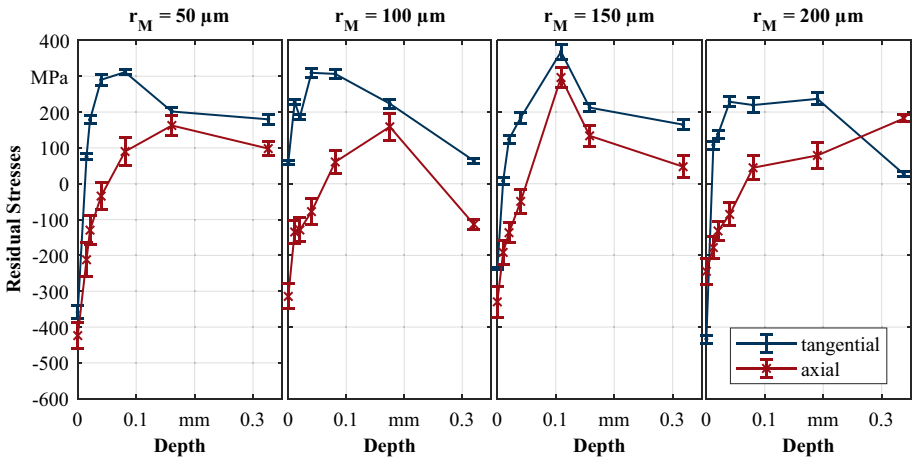

Fig. 8 Residual stress depth profiles measured at the contact point of the 30°-tangent to the tooth root fillet

$r_M = 200\,\mu$m, the tangential surface residual stresses are ca. 360ldots -430 MPa. For $r_M = 100\,\mu$m, the tangential residual stresses are slightly tensile (ca. 60 MPa).

The axial residual stresses at the surface (in Fig. 8) show significant deviations compared to the measurements on the uncut gear in the tooth ground (in Fig. 7). The deviations can be caused by cutting of the gear tooth close to the measuring point. The cutting possibly has affected the near surface residual stress state in the present case. This has not been observed for case-hardened materials but is possible for this lower strength material, where a relaxation of the residual stresses is more likely.

Additional measurements on the gear flank, where the cut is placed further away from the measuring point (compare Fig. 3) are therefore also evaluated. For the variants with $r_M = 50\,\mu$m and $r_M = 200\,\mu$m, additional measurements on the tooth flank were performed. For these measurements at the tooth flank, influences of the cutting process on the residual stresses are unlikely because the cut is placed in ca. 10 mm distance to the measuring point (see Fig. 3).

In Fig. 9, it can be seen that, the axial residual stresses for $r_M = 200\,\mu$m are ca. -590 MPa and are significantly higher than for $r_M = 50\,\mu$m with ca. -310 MPa. Furthermore, these measurements are better comparable to the measurements on the uncut gears. The surface tangential residual stresses on the tooth flank are ca. -60 MPa for $r_M = 50\,\mu$m and ca. -485 MPa for $r_M = 200\,\mu$m. In larger material depth, the residual stresses at the tooth flank behave similar to the residual stresses in the 30°-tangent of the tooth root.

The different measurements indicate higher axial and tangential surface residual stresses for a larger die edge radius in the range of $r_M = 50 \ldots 200\,\mu$m. The compressive residual stresses are close to the cut surface and the transition to tensile stresses is in material depths of ca. 0.01 . . . 0.05 mm. For tooth root breakage, both the tangential and axial surface or near surface residual stresses should be relevant due to the complex stress condition, which is caused by the notch effect of the tooth root [18,39].

For the measurement of these residual stresses, a cut near the measurement point was necessary, which possibly lead to a change in the residual stresses. The reason for this assumption is that the surface compressive

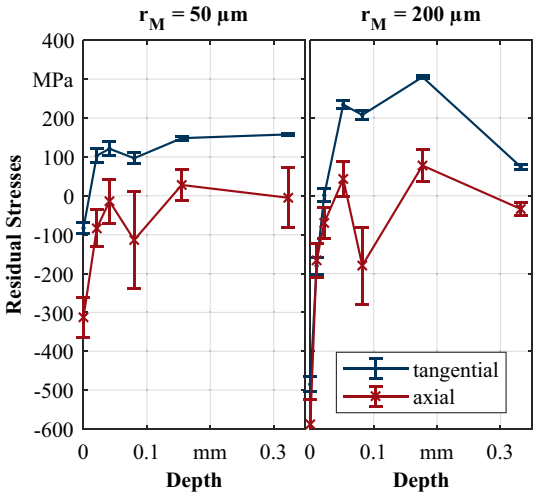

Fig. 9 Residual stress depth profiles measured at the tooth flank (pitch point)

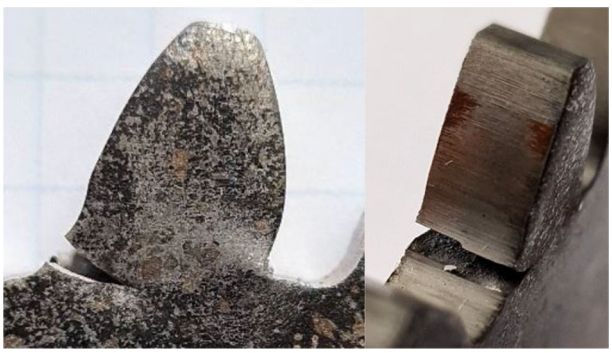

Fig. 10 Exemplary photograph of the occurred tooth root breakages

residual stresses (in Fig. 8) show no increase for larger die edge radii, which was observed in previous studies. The measurement of the axial residual stresses (in Fig. 7) shows this relation as well as the measurements at the tooth flank (in Fig. 9). However, the tangential residual stresses in the area of the 30°-tangent could not be determined instead the measurement of axial residual stresses in the tooth fillet and the comparable axial residual stresses at the tooth flank indicate that the residual stresses are comparable on the cut surface. This leads to the statement that the residual stresses in Fig. 7 roughly represent the axial and tangential residual stresses on the cut surface.

3.4 Fatigue testing—tooth root bending strength

The stress-cycle (S–N) curve was determined on the pulsating test rig. In the limited lifetime range, 5 test runs were performed on each of the two pulsating force load stages 10 kN and 8.5 kN. The endurance limit was determined by 13 tests with 5.5…7 kN pulsating force.

The observed breakages show typical characteristics of tooth root breakage. The cracks initiate at the surface at the 30°-tangent. The cracks also seem to be initiated evenly over the whole tooth width. After the crack initiation, the crack grows within few load cycles until the pulsating test rig is stopped due to the set maximum distance limits. The tooth does not break off with a final rupture as usually observed on case-hardened gears. This is due to the relatively high ductility of this material compared to case-hardened gears. An exemplary breakage is shown in Fig. 10.

An influence of the burr was assumed due to the research results of milled gears in FVA 284 IV [22] and therefore investigated by deburring and testing a gear. For the three test runs in the limited lifetime, no significant deviation in the endured number of load cycles was observed.

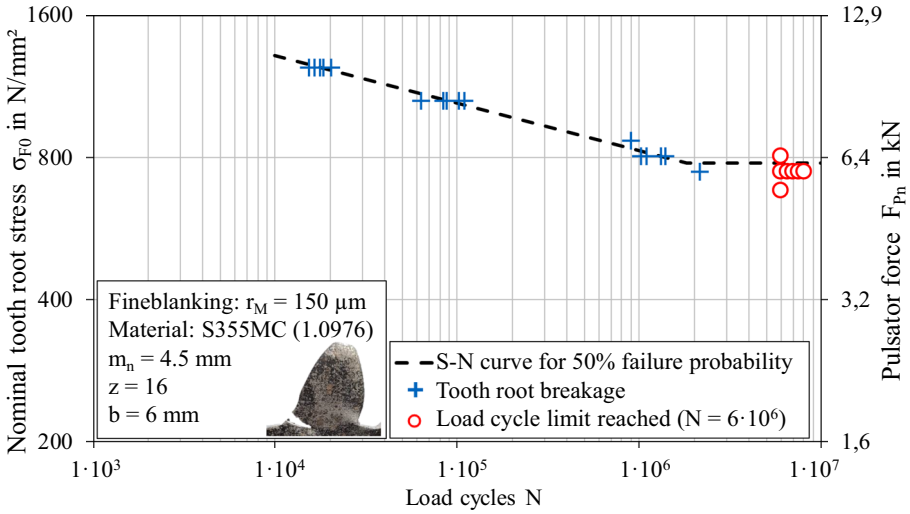

Fig. 11 S–N curve for tooth root bending for 50% failure probability of the fineblanked gear with a die edge radius of $r_M = 150\,\mu$m

Table 5 Calculation factors for nominal tooth root stress, nominal stress number (bending) and allowable stress number

Denomination	Symbol	Test gear
Gear tested over (number of teeth)	k	3
Load direction angle	α_{Fn}	22.5°
Bending lever arm	h_{Fn}	5.12 mm
Tooth root chord at the critical section (30°-tangent)	s_{Fn}	8.766 mm
Tooth root radius at the critical section (30°-tangent)	ρ_F	1.795 mm
Conversation factor $F_{Pn} \rightarrow \sigma_{F0}$ *	C	0.124 1/ mm²
Conversion factor from 50 to 1% failure probability	$f_{1\%F}$	0.92
Stress correction factor	Y_{ST}	2.0
Life factor	Y_{NT}	1.0
Test relative notch sensitivity factor	$Y_{\delta relT}$	0.998
Relative surface factor	Y_{RrelT}	1.006
Size factor	Y_X	1.0

*Valid for the herein selected pulsator clamping

In Fig. 11, the determined S–N curve for 50% failure probability is shown for the variant with a die edge radius $r_M = 150\,\mu$m. This variant was investigated first. All further variants are tested currently and their results will be presented within an additional publication.

The nominal tooth root stress σ_{F0} is calculated for the manufactured gear geometry as shown in Fig. 4 with the factors shown in Table 5. With the determined conversion factor C of this test gear, as listed in Table 5, the pulsating force can be converted in the nominal tooth root stress for a 50% failure probability with Eq. 3.

$$\sigma_{F0} = C \cdot F_{Pn}. \tag{3}$$

The determined nominal tooth root stress for endurance strength with 50% failure probability is $\sigma_{F0\infty,50\%,pulsator}$=776 N/mm² for the fineblanked gear with $r_M = 150\,\mu$m. This corresponds to a pulsator force of $F_{Pn50\%}$ = 6.25 kN.

For the calculation of the stress numbers with Eqs. 1 and 2, all Y-factors are calculated according to ISO 6336-3 [14] for steel (St) with yield stress σ_S = 400 N/mm². Therefore, the slip layer thickness is ρ' = 0.0445 mm. The Y-factors are also listed in Table 5.

The determined reference stress numbers for 1% failure probability are calculated with the factor $f_{1\%F}$ = 0.92 for blasted gears, which is used usually to take into account a peening process or the residual stresses state according to Niemann/Winter [31]. In this case, the process-induced residual stresses are considered with this factor. The stress correction factor, relevant to the dimensions of the reference test gears is Y_{ST} = 2.0. The stress numbers determined in pulsating test rigs differ from the stress numbers determined in

running test rigs due to the statistics of failure probability [31]. The conversion from pulsating tests to running tests is done with the factor $f_P = 0.9$ according to [5].

The determined allowable stress number for bending is $\sigma_{FE,test} = 640\,N/mm^2$ and the nominal stress number for bending is $\sigma_{Flim,test} = 320\,N/mm^2$. These determined strength numbers can be compared to test results of reference gears stated in ISO 6336-5 [15].

Compared to wrought normalized carbon steels, which have strength numbers of ca. 120…230 N/mm^2 depending on the quality, these fineblanked gears have a significantly higher tooth root bending strength.

Compared to case carburized gears (ca. 310…530 N/mm^2), these fineblanked gears would correspond to material quality ML or lower. However, there are test results of unpeened case-hardened gears with comparable strength numbers in [5] with $\sigma_{Flim} = 250…350\,N/mm^2$. For case-hardened blast cleaned gears of 16MnCr5 a bending strength of $\sigma_{Flim} = 430\,N/mm^2$ is stated in [24].

In VDI 2736 [38], the bending strength numbers for the plastic gear materials POM and PA66 are stated. At room temperature, the bending strength numbers are $\sigma_{FlimN,POM} = 35\,N/mm^2$ and $\sigma_{FlimN,PA66} = 31\,N/mm^2$. The tooth bending strength for sintered (laser beam melted) gears out of the material 16MnCr5 is $\sigma_{Flim,test} = 309\,N/mm^2$ in [16].

Consequently, it can be stated that the herein investigated fineblanked gears have a tooth root bending strength that:

- Exceeds by far the bending strength numbers of commonly used plastic materials,
- Is significantly higher compared to gears made of wrought normalized carbon steels,
- Is comparable to sintered gears resp. case-hardened, unpeened gears,
- Is below the tooth root bending strength of blast cleaned or shot peened case-hardened gears.

4 Summary and conclusion

The pinion of a gearing was fineblanked out of 6-mm-thick sheet metal made of S355MC. Sections of the gear were fineblanked with four variations of the die edge radius r_M. The fineblanked gear was investigated regarding the manufactured geometry, the hardness, the flank surface roughness and the process-induced residual stresses. Further, fatigue tests regarding tooth bending strength were performed with a standard pulsating test rig. The S–N curve for one variant was determined and the tooth root bending strength numbers according to ISO 6336-5 [15] are stated.

The different die edge radii do not significantly alter the cut surface characteristics and hardness distribution in the tooth root. For all variants, a very high clean cut share of over 98% of the sheet thickness was observed. For the four variants, an increase in surface hardness from ca. 150 HV up to 330 HV was observed, with all variants showing a comparable hardness distribution.

The cut surface roughness is ca. Ra = 1.36 to 1.77 μm which is significantly higher than that of milled gears. Surprisingly, a clear dependency between the die edge radius and the roughness Ra was observed, where a bigger radius leads to a higher roughness.

The fineblanked gear geometry was measured and evaluated regarding the accuracy or quality grade of the gear. The investigation shows that it is possible to manufacture gears with a very high precision with fineblanking comparable to gear hobbing.

For the variant with $r_M = 150\,\mu m$, a first S–N curve was determined, which is used to classify the tooth root bending strength of the fineblanked gears. The nominal stress number for bending in the test is ca. $\sigma_{Flim,test} = 320\,N/mm^2$, which is in the area of low-quality case-hardened gears but significantly higher than for plastic materials or wrought normalized carbon steels. However, these fineblanked gears are manufactured in one step with a "simple" steel, which is much more cost-effective. Only the production costs of plastic gears are comparable to the manufacturing costs of these fineblanked gears, which usually have ca. one-tenth of the tooth root bending strength.

This research shows the potential of using shear cutting processes such as fineblanking for manufacturing gears or other complex geometries with functional surfaces. The costs of the manufacturing are comparable to plastic gears but the fatigue strength can be much higher.

In the future, the S–N curves of the variants with different die edge radii need to be determined to investigate the influence of the residual stresses on the tooth root bending strength for this material. The material used in this research for fineblanking of the gears is a ductile steel with low strength compared to usually used gear materials. By fineblanking gears out of higher-strength materials, the tooth root bending strength can possibly be further increased. Additionally, in this case the positive effect of the compressive residual stresses

is expected to be greater due to higher residual stress sensitivity. Furthermore, the flank load carrying capacity regarding pitting will be investigated for the fineblanked gears in the further course of the research project.

Acknowledgements This work is funded by the Deutsche Forschungsgemeinschaft (DFG, German Research Foundation)—VO 1487/30-1; VO 1487/30-2; STA 1198/13-1; STA 1198/13-2 and is part of the DFG-priority program https://www.utg.mw.tum.de/spp-2013/SPP2013. The residual stresses measurement with the PULSTEC μ-X360s was made possible by Sentenso GmbH, who provided the X-ray diffractometer.

Funding Open Access funding enabled and organized by Projekt DEAL.

Compliance with ethical standards

Conflicts of interest The authors declare that they have no conflict of interest.

References

1. Česnik, D., Bratus, V., Kosec, B., Bizjak, M.: Distortion of ring type parts during fine-blanking. Metalurgija **51**, 157–160 (2012)
2. DIN 3960: Definitions, parameters and equations for involute cylindrical gears and gear pairs (1987)
3. DIN 3961: Tolerances for cylindrical gear teeth; basis (1978)
4. DIN 3990: Calculation of load capacity of cylindrical gears (1987)
5. Dobler, F., Tobie, T., Stahl, K.: Influence of low temperatures on material properties and tooth root bending strength of case-hardened gears. In: Volume 10: ASME 2015 Power Transmission and Gearing Conference; 23rd Reliability, Stress Analysis, and Failure Prevention Conference. ASME (2015). https://doi.org/10.1115/DETC2015-46325
6. Elyasi, M.: An investigation on the parametric analysis of v-ring indenter mechanism in fine-blanking process. Int. J. Mech. Appl. **3**(4), 76–80 (2013)
7. Güntner, C., Tobie, T., Stahl, K.: AGMA 2017 Fall Technical Meeting, chap. Influences of the residual stress condition on the load carrying capacity of case hardened gears, pp. 328–344. Columbus, Ohio, USA (2017)
8. Gupta, K., Jain, N.K., Laubscher, R.: Chapter 4—Advances in gear manufacturing. In: Gupta, K., Jain, N.K., Laubscher, R. (eds.) Advanced gear manufacturing and finishing, pp. 67–125. Academic Press, London (2017). https://doi.org/10.1016/B978-0-12-804460-5.00004-3
9. Haibach, E.: Betriebsfestigkeit: Verfahren und Daten zur Bauteilberechnung, 3, korrigierte und erg. Aufl VDI-Buch. Springer, Berlin (2006)
10. Höhn, B.R., Oster, P., Michaelis, K., Suchandt, T., Stahl, K.: Bending fatigue investigation under variable load conditions on case-carburized gears. In: AGMA 2000 Fall Technical Meeting (2000)
11. Hück, M.: Ein verbessertes Verfahren für die Auswertung von Treppenstufenversuchen. Z. Werstofftechnik **14**, 406–417 (1983)
12. ISO 4287: Geometrical product specifications (GPS)–surface texture: Profile method—terms, definitions and surface texture parameters (1997)
13. ISO 6336: Calculation of load capacity of spur and helical gears (2006)
14. ISO 6336-3: Calculation of load capacity of spur and helical gears: Calculation of tooth bending strength (2006)
15. ISO 6336-5: Calculation of load capacity of spur and helical gears: strength and quality of materials (2003)
16. Kamps, T., Schmidt, M., Siglmüller, F., Winkler, J., Schlick, G., Seider, C., Tobie, T., Stahl, K., Reinhart, G.: Laser beam melting of 16MnCr5 and resulting material properties. Addit. Manuf. **35**, 101372 (2020)
17. Kim, J.D., Kim, H.K., Heo, Y.M., Chang, S.H.: A study on the relation between die roll height and die chamfer shape in fine blanking for special gear. In: Key Engineering Materials and Computer Science, Advanced Materials Research, vol. 320, pp. 92–96. Trans Tech Publications Ltd (2011). https://doi.org/10.4028/www.scientific.net/AMR.320.92
18. Kleemann, U., Zenner, H.: Bauteiloberfläche und schwingfestigkeit—untersuchungen zum einfluss der randschicht auf die dauerschwingfestigkeit von bauteilen aus stahl. Materialwiss. Werkstofftechn. **37**(5), 349–373 (2006). https://doi.org/10.1002/mawe.200600995
19. Klocke, F.: Sheet Metal Separation, pp. 407–456. Springer, Berlin (2013)
20. Lara, A., Picas, I., Casellas, D.: Effect of the cutting process on the fatigue behaviour of press hardened and high strength dual phase steels. J. Mater. Process. Technol. **213**, 1908–1919 (2013)
21. Maronne, E., Galtier, A., Robert, J.L., Ishikawa, T.: Cutting process influence on fatigue steel sheets properties. WIT Transactions on Engineering Sciences **40**, 13-22 (2003)
22. Matt, P., Tobie, T.: Einfluss der Stirnkante auf die Tragfähigkeit von Zahnrädern unter Berücksichtigung des Schrägungswinkels FVA-Nr. 284/IV- Heft 1023 (2012)

23. Müller, D., Stahl, J., Pätzold, I., Golle, R., Tobie, T., Volk, W., Stahl, K.: Influence of shear cutting process parameters on the residual stress state and the fatigue strength of gears. ICTP Ohio (Preprint) (2020). https://doi.org/10.31224/osf.io/t4wbq
24. Niemann, G., Winter, H.: Maschinenelemente Band 2: Getriebe allgemein, Zahnradgetriebe - Grundlagen, Stirnradgetriebe. Springer, Berlin (2002)
25. Rettig, H.: Ermittlung von zahnfußfestigkeits-kennwerten auf verspannungsprüfständen und pulsatoren. Antriebstechnik **26**(2), 51–55 (1987)
26. Schmidt, R., Hellmann, M., Burkhard, R., Rademacher, P., Höfel, P., Birzer, F., Hoffmann, H.: Cold Forming and Fineblanking, 2nd edn. Carl Hanser Verlag, München Wien (2007)
27. Schmitt, M., Kamps, T., Siglmüller, F., Winkler, J., Schlick, G., Seidel, C., Tobie, T., Stahl, K., Reinhart, G.: Laser-based powder bed fusion of 16MnCr5 and resulting material properties. Addit. Manuf. **35**, 101372 (2020). https://doi.org/10.1016/j.addma.2020.101372
28. Spišák, E., Majerníková, J., Spišáková, E.: The influence of punch-die clearance on blanked edge quality in fine blanking of automotive sheets. Mater. Sci. Forum **818**, 264–267 (2015). https://doi.org/10.4028/www.scientific.net/MSF.818.264
29. Stahl, J., Müller, D., Pätzold, I., Golle, R., Tobie, T., Volk, W., Stahl, K.: The influence of residual stresses induced by near-net-shape blanking processes on the fatigue behavior under bending loads. In: IDDRG Conference Proceedings (2019)
30. Stahl, J., Müller, D., Tobie, T., Golle, R., Volk, W., Stahl, K.: Production engineering. In: Chap. Residual stresses in parts manufactured by near-net-shape-blanking. Springer, Berlin (2018). https://doi.org/10.1007/s11740-018-0865-5
31. Stahl, K.: Lebensdauerstatistik FVA-Nr. 304 II - Heft 580 (1999)
32. Stenico, A., Krug, T.: Eigenspannungen Zahnfuß FVA-Nr. 369 I+II - Heft 745: Eigenspannungseinfluss auf die Zahnfuß-tragfähigkeit kleinmoduliger Zahnräder (2004)
33. Su, C., Dong, X., Guo, S., Li, Q., Li, T.: Research on parameters optimization of bilateral ring gear blank-holder in thick-plate fine blanking. Frattura Integr. Strutt. **30**, 502–514 (2014). https://doi.org/10.3221/IGF-ESIS.30.61
34. Tekiner, Z., Nalbant, M., Gürün, H.: An experimental study for the effect of different clearances on burr, smooth-sheared and blanking force on aluminium sheet metal. Mater. Des. **27**(10), 1134–1138 (2006)
35. Thipprakmas, S., Chanchay, C., Hanwach, N., Wongjan, W., Vichitjarusgul, K.: Investigation on the increasing material hardness on fineblanked sprocket. In: Advances in Materials and Processing Technologies, *Advanced Materials Research*, vol. 83, pp. 1099–1106. Trans Tech Publications Ltd (2010). https://doi.org/10.4028/www.scientific.net/AMR.83-86.1099
36. Tobie, T., Matt, P.: FVA directive 563 I: Standardisation of load capacity tests (2012)
37. Townsend, D.P., Zaretsky, E.V.: Effect of shot peening on surface fatigue life of carburized and hardened aisi 9310 spur gears. NASA Technical Paper (1982)
38. VDI 2736-2: Thermoplastische Zahnräder (2014)
39. Weber, R.: Auslegungskonzept gegen volumenversagen bei einsatzgehärteten stirnrädern. Dissertation, Universität Kassel (2015)
40. Yasutomi, T., Yonemura, S., Yoshida, T., Mizumura, M., Hiwatashi, S.: Blanking Method with Aid of Scrap to Reduce Tensile Residual Stress on Sheared Edge, vol. 896. IOP Publishing, Bristol (2017)